Indirect structural health monitoring in bridges: scale experiments

F. Cerda[1,], J.Garrett [1], J. Bielak [1], P. Rizzo [2], J. Barrera [1], Z. Zhuang [1], S. Chen [1], M. McCann [1] & J. Kovačević [1]

[1] Carnegie Mellon University, Pittsburgh, Pennsylvania, USA

[2] University of Pittsburgh, Pittsburgh, Pennsylvania, USA

ABSTRACT:

In this paper, we use a scale model to experimentally validate an indirect approach to bridge structural health monitoring (SHM). In contrast to a traditional direct monitoring approach with sensors placed on a bridge, the indirect approach uses instrumented vehicles to collect data about the bridge. Indirect monitoring could offer a mobile, sustainable, and economical complementary solution to the traditional direct bridge SHM approach. Acceleration signals were collected from a vehicle and bridge system in a laboratory-scale experiment for four different bridge scenarios and five speeds. These signals were classified using a simple short-time Fourier transform technique meant to detect shifts in the fundamental frequency of the bridge due to changes in the bridge condition. Results show near-perfect detection of changes when this technique is applied to signals collected from the bridge (direct monitoring), and promising levels of detection when one uses signals from sensors on the vehicle (indirect monitoring) instead of those recorded on the bridge itself.

1 INTRODUCTION

In this paper, we explore whether the acceleration signals from vehicles moving over a bridge can be used for diagnostic purposes. The acceleration signals from the bridge and the vehicle are affected mainly by three different factors. These factors are: the dynamic properties of the bridge structure; the motion characteristics of the passing vehicle; and the dynamic properties from the vehicle.

Traditionally, the Structural Health Monitoring (SHM) community uses the data measured *directly* from a structural system for diagnostic purposes. In such an approach, a number of sensors are deployed on the structure. We refer to this as a *direct* SHM approach. In contrast, the use of data not recorded directly from a structure is referred to as an *indirect* SHM approach (Lin et al. 2005, Cerda et al. 2010). The top block in Figure 1 shows this distinction in terms of the data acquisition approach.

There are several practical reasons that drive our research on the *indirect* SHM approach. There is a need in most countries, and especially in the US, to monitor a large bridge stock in a reliable, objective and economically feasible way. The traditional *direct* SHM approach requires installation, power and maintenance of an expensive electronic infrastructure on top of the physical bridge infrastructure.

The indirect approach can gain leverage by using the equipment already located on board newer models of vehicles, or on a fleet of vehicles that can be equipped with sensors to collect the desired information as they undergo their daily routines.

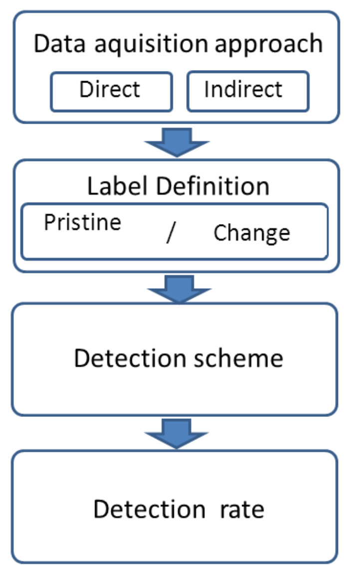

Figure 1. Block diagram of proposed system

The *indirect approach,* however, has the disadvantage that the data are influenced by the motion of the vehicle and its dynamic properties.

Through the use of an experimental setup which is described in the next section, we collected acceleration data from a particular scale bridge structure and a particular scale vehicle in order to compare the *indirect* and *direct* methods. These two data acquisition approaches are depicted in the first block of Figure 1 since both approaches for SHM were tested as part of the experiments described in this paper. As far we know, such comparisons have not been carried out previously.

To test the detection capability of the different approaches, we created four experimental scenarios. The first scenario considers the structure in a pristine while in each of the other three, we added mass to the bridge to simulate damage. Two different scenarios are compared in each test. A pristine one, and a second one with the induced change to modify its dynamic properties. The second block in Figure 1 shows the two scenarios considered.

The data from the two scenarios is classified by means of a short-time Fourier transform-based change detection scheme aimed at detecting changes in the fundamental frequency of a bridge. We report the results of this work in terms of the detection rate. This quantity reflects the fraction of cases in which an actual change is detected. These two steps are represented in the last two blocks in Figure 1.

Previous work includes a theoretical solution for the simplified case of a single degree of freedom oscillator travelling over a beam structure (Yang et al. 2004). In a subsequent paper, Lin et al. (2005) were able to experimentally determine the natural frequency of an actual bridge structure by analyzing the acceleration signals of a passing vehicle.

An experimental setup was used by Kim to simulate the vehicle-bridge interaction and identify damage scenarios (Kim et al. 2010). A particular methodology, referred as the "pseudo static approach", was used to identify damage using vibration data taken from the bridge structure at different locations along the bridge span (¼, ½ and ¾ of span length). This damage identification approach shows good accuracy at determining a change of stiffness of the bridge. Being inspired by this experimental work, we decided to further pursue the identification of changes in the bridge structure using the indirect approach.

In this paper, we concentrate on studying the influence of different vehicle velocities and sensor locations on the classification accuracy of different scenarios. The scenarios are produced in a laboratory using a scaled physical model of a moving vehicle over a simply supported bridge. The data is obtained through multiple runs of the vehicle over the structure. Hereafter, we refer to this particular experimental setup as the "scale bridge structure".

The following section contains a description of the experimental setup. This description includes the structural model, the vehicle model, the vehicle motion control system, and the data acquisition equipment. The third section contains a description of the different scenarios that were compared in the detection experiments. In the fourth section, we describe the Fourier transform-based change detection approach, and in the fifth section, we present and discuss preliminary results. Our initial conclusions are given in the last section.

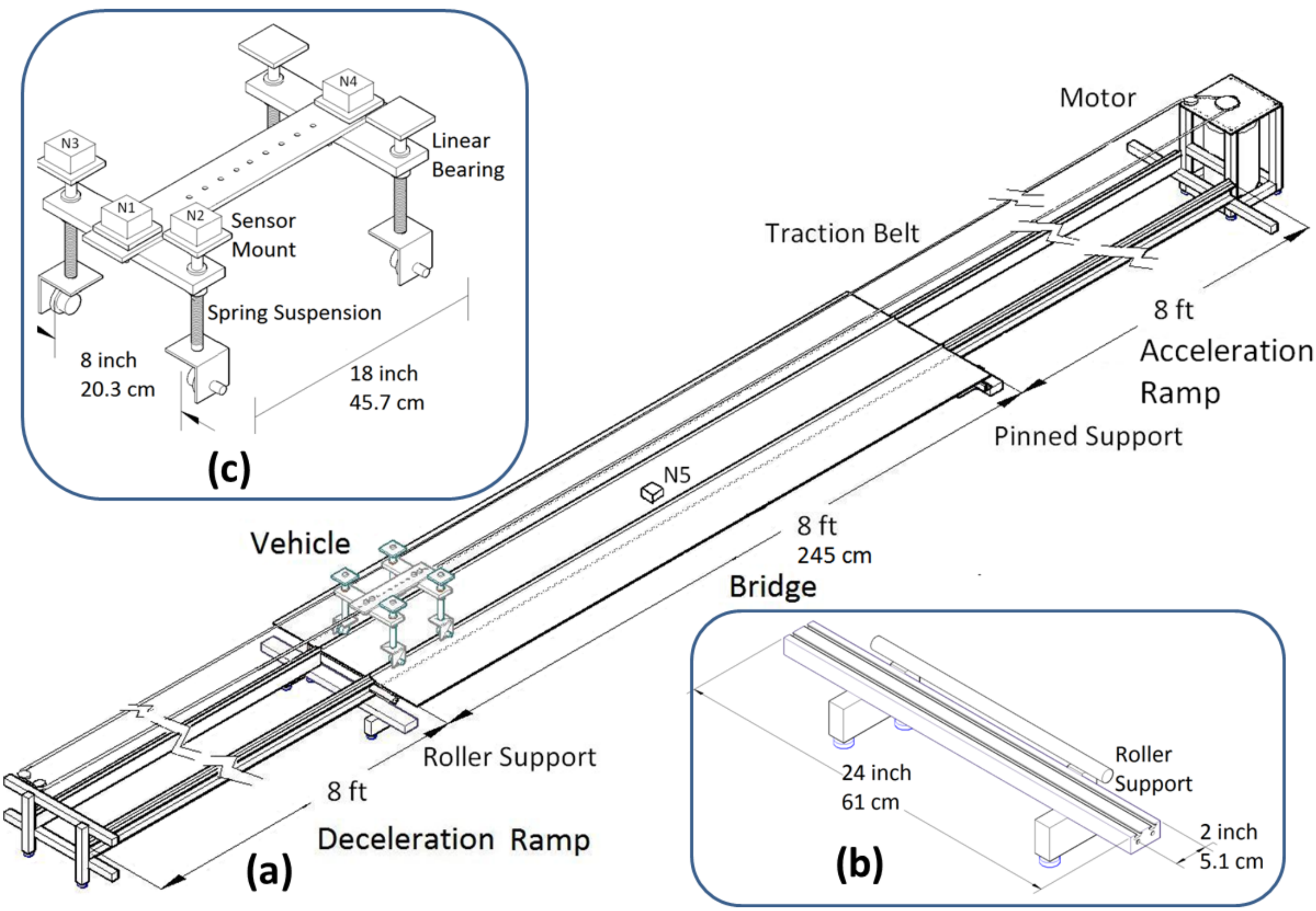

Figure 2. Structural components and vehicle from experimental setup

2 EXPERIMENTAL SETUP

The experimental setup simulates a passing vehicle over a simply supported bridge structure. The vehicle-bridge interaction is studied by recording accelerations at four different locations on the vehicle as well as at the midspan of the bridge. The whole system consists of several components: 1) the mechanical components consisting of the bridge, its approaches, and the vehicle, 2) the vehicle motion control system and 3) the data acquisition system.

2.1 *Mechanical components*

An overview of the mechanical components is given in Figure 2 (a). It consists of an acceleration ramp and a deceleration ramp that provide the running path for the vehicle, and a simply supported bridge. The acceleration and deceleration ramp are made from C Shape aluminum extrusions (2 x 1 x 1/8 in). They are supported on each end by aluminum slotted extrusions. The slotted extrusion shown in Figure 2 (b) allows one to fix the ramps at different locations along the slots. This flexibility will allow further research that will explore placing the ramps in the right or left lanes to study the effect of traffic-induced torsion.

2.1.1 *Vehicle*

The vehicle used on the experiment has two axles. A scheme of the vehicle is shown in Figure 2(c). The vehicle has four independent wheel suspensions. In this paper the vehicle properties are maintained at constant values shown in Table 1. The dynamic properties of the vehicle were obtained by capturing the dynamic response after an impulse force is applied.

Table 1. Vehicle properties

Properties with added mass	
Bouncing frequency	5 Hz
Front damping	5.9%
Rear damping	5.9%
Extra weight at midspan	5 lb)

The suspension system is designed so it can be easily modified to simulate different vehicle characteristics. For example, a heavily loaded 2 axle vehicle can be simulated by replacing the spring in the suspension shown in Figure 2(c) with a stiffer spring.

2.1.2 *Bridge*

The bridge structure is composed of an aluminum plate and two aluminum angles that act as beams. A cross-sectional view of the bridge is shown in Figure 3.

.

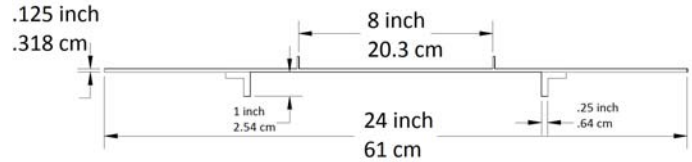

Figure 3. Bridge section

The bridge deck also has two angles on top that are used as rails for the vehicle. The properties of the bridge are shown in Table 2.

Table 2. Bridge properties

Deck dimensions	8 x 2 x 1/8 in
Beams dimensions	8 x 1 x 1/4 in
Fundamental frequency	7.18 Hz
Damping	1.35%

2.2 *Motion control*

A set of National Instrument® components was configured to reliably control the speed of the vehicle. The individual components are shown in Figure 4. The PXI 7342 motion controller commands the NI 70360 driver that provides the signals to a double shaft stepper motor, model NEMA 34. The encoder attached to the shaft of the motor provides position feedback and closes the loop for the motion control system.

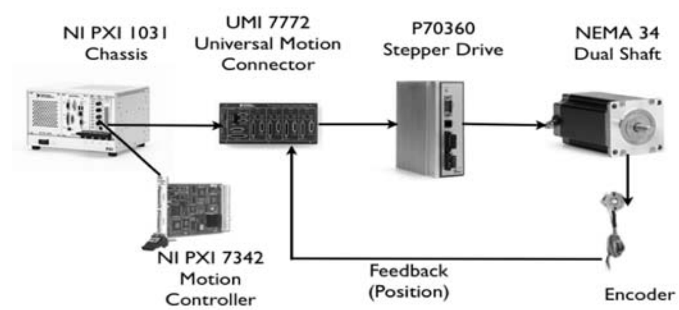

Figure 4.Motion control equipment scheme (Images from www.ni.com)

A list of the individual components is shown in the Table 3.

Table 3. Motion equipment components

Driver	NI 70360
Motor	NEMA 34
Motion Controller	NI PXI 7342
Interface	UMI 7772

2.3 *Data acquisition equipment*

The data acquisition system for the moving vehicle and bridge is wireless. Figure 5 shows the Microstrain® acceleration sensor nodes that communicate to a base directly connected to the PXI controller. The data is transmitted in packets to the base after digitalization. The resolution of the acceleration data is 1.5mg RMS. The resolution of the digitization is 12 bit.

The components used in the data acquisition process are described in Table 4.

Table 4. Data acquisition components

Acceleration nodes	MicroStrain G-Link mXrs 2G
Wireless base	MicroStrain WSDA mXrs

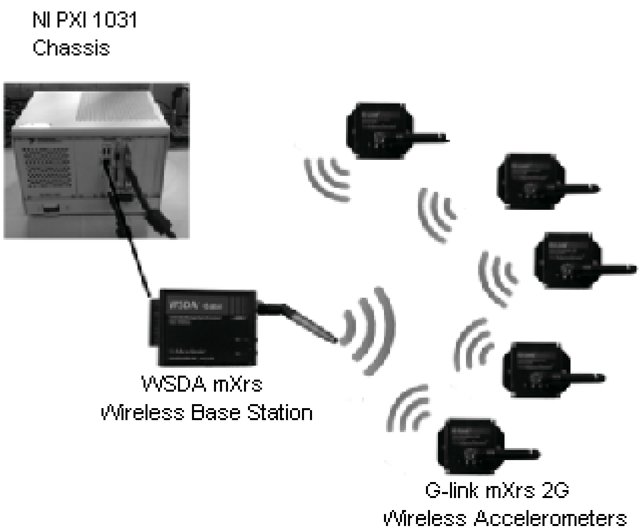

Figure 5. Data acquisition equipment

The sensor on the bridge is located at the center of the midspan, as depicted in Figure 2 (a) by the node labeled N5. The vehicle sensor locations are labeled as N1, N2, N3, and N4 in Figure 2 (c). Table 5 lists the sensor locations and the corresponding node names shown in Figure 2 (a) and (c).

Table 5. Node location

Node Name	Node location
N1	Front Suspension Front
N2	Left Wheel front
N3	Right Wheel front
N4	Rear Suspension
N5	Bridge

The nodes located at the top of the suspension shaft, N2 and N3, transmit the vertical motion at the wheel level through the suspension shaft.

3 EXPERIMENTAL SCENARIOS

In the work of Yang et al (2004), the authors derived an explicit analytical solution for the interaction of a simply supported beam with a traveling single degree of freedom oscillator. In this solution, the main interaction parameters are defined as S and μ: (1) $S = \pi v/L\omega_b$;(2) $\mu = \omega_b/\omega_v$, where S is a normalized vehicle velocity; v = vehicle velocity; ω_v = the vehicle (oscillator) vertical natural frequency; L = length of beam, and ω_b= fundamental natural frequency of the beam.

We explored the influence of these parameters by inducing changes to the bridge structure and running the moving vehicle at different travelling speeds over the bridge. The bridge was changed by adding mass at the midspan. Figure 6 shows the procedure by which different amounts of mass were clamped at the midspan of the bridge. For our structure, ω_b is the fundamental natural frequency of the complete bridge system.

The different conditions of the bridge and the corresponding changes that they produce in terms of the fundamental frequency of the bridge are summarized in Table 6.

Table 6. Bridge scenarios

Scenario	Total added mass (lbs, % of bridge mass)	fundamental freq (Hz)
1	0, 0%	7.18
2	6, 16%	6.28
3	10, 27%	5.93
4	14, 38%	5.57

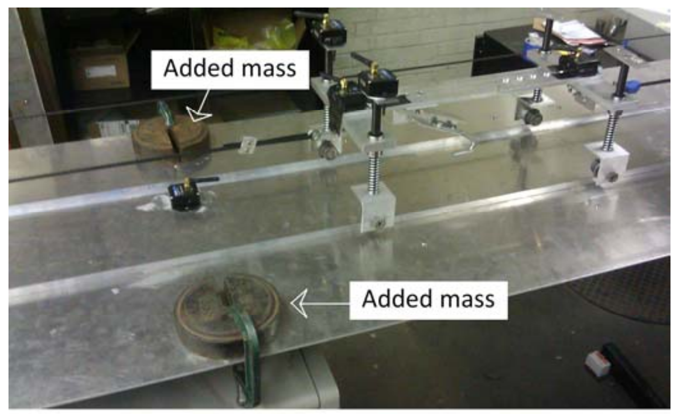

Figure 6. Added mass to the midspan of the experimental bridge structure.

The speed of the vehicle under the different bridge scenarios ranged from 1 m/s to 3 m/s at 0.5 m/s intervals. A total of 5 different speeds were studied.

The range of scenarios and speeds can be plotted in terms of the parameters S and μ as depicted in Figure 7.

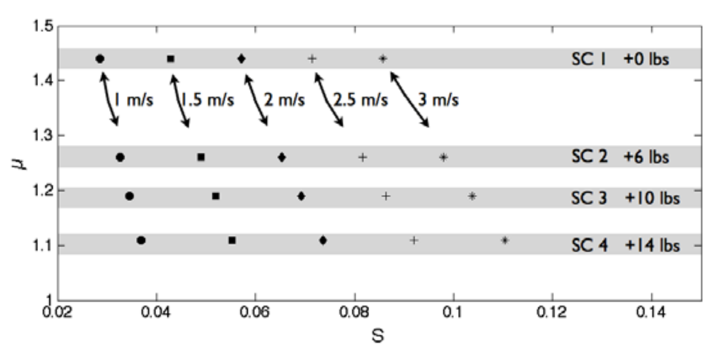

Figure 7. S and μ cases studied experimentally.

Each of the 20 dots in Figure 7 reflects a data set composed of 60 runs of the vehicle over the bridge. We compare the variation of the different data sets by performing detection experiments, as described in the next section.

4 DETECTION OF STRUCURAL SCENARIOS

The detection task is as follows. First, we use a training set of acceleration signals from a vehicle traveling over a known-to-be-healthy (pristine) scale bridge structure to set a baseline for the system. We then use a test set of different acceleration signals from the same bridge under different scenarios, to determine if the detection approach can detect whether the bridge has sustained a significant change since the collection of the training set. For the specific scenarios we are exploring, note that the induced change causes a decrease in the fundamental frequency of the bridge. We therefore hypothesize that a classification scheme based on detecting shifts in this frequency should work well.

Figure 8 shows a typical signal obtained through the experimental setting and the corresponding portion of the signal used for the classification, which is when the vehicle is completely between the supports of the bridge.

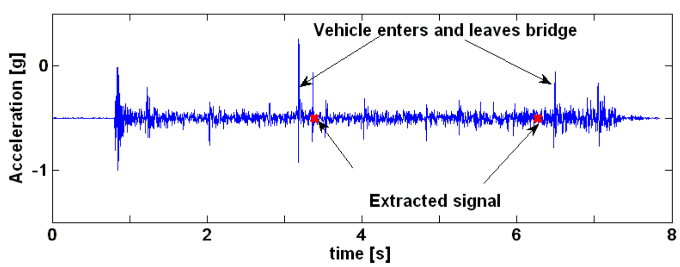

Figure 8 Original acceleration signal.

4.1 *STFT Calculation.*

To detect changes in the bridge, we first extract the frequency spectrum of the bridge/vehicle system from an acceleration signal. As seen in Figure 9, taking the Fourier transform of the acceleration signal results in a frequency spectrum with a large amount of noise and little consistency between runs; this is because the time-domain signal contains numerous spikes and other transient signals. We instead compute the spectrogram of the acceleration signal with a short-time Fourier transform (STFT) with overlapping windows that are 250 samples in length. The spectrogram is shown in Figure 10. We then average the spectrogram over time, creating a frequency spectrum as depicted in Figure 11. This technique exploits the fact that the frequencies of interest are not transient, while much of the noise is. The time averaging should therefore remove noise and preserve the signal.

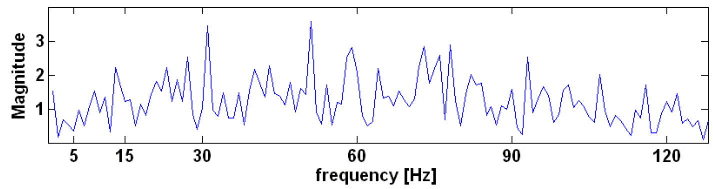

Figure 9. Fourier transform of an acceleration signal.

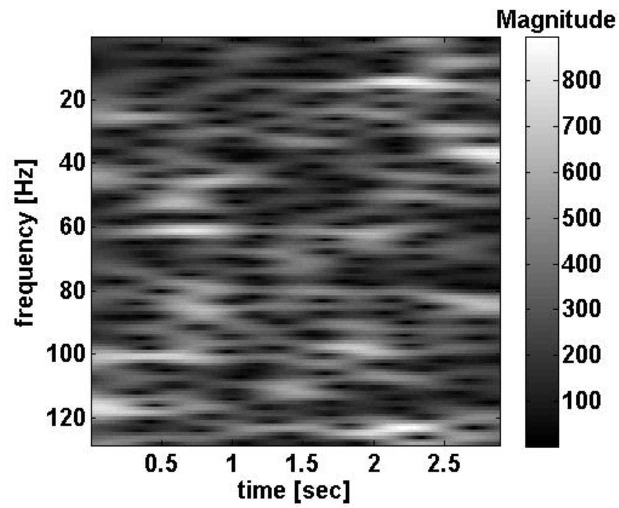

Figure 10. Acceleration spectrogram.

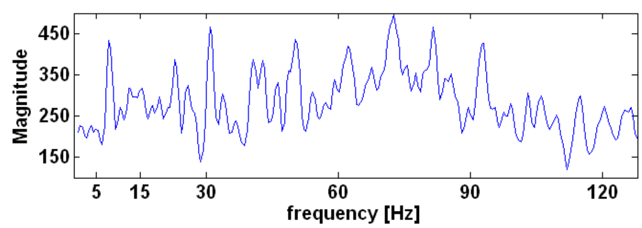

Figure 11. Spectrogram averaged across time.

4.2 *Classification System.*

For the training of our classification system, the data from each scenario at a particular speed is divided into training and testing sets. The spectrum of each signal in the training set is calculated first, then all such signals are averaged across frequency. The result is a single reference spectrum representing the undamaged bridge. To determine whether a testing set of signals indicates a change in the structure, the spectrum is computed for each signal in the testing set and again averaged across frequency to create a signal candidate spectrum for each scenario at a particular speed. The portion of each spectrum corresponding to the range 3.5-13 Hz is then extracted. The averaged candidate spectrum with the corresponding extracted section is shown in Figure 12.

The considered range is where our theoretical calculations suggest the fundamental frequency of the bridge should appear, and experimental exploration confirms it. Finally, the trimmed reference and candidate spectra are shifted to be zero mean and their cross-correlation is computed. If the maximum value of the cross-correlation occurs when the spectra are not shifted, then the test set is labeled as unchanged. If the maximum value occurs at a shifted location, the test set is labeled as changed.

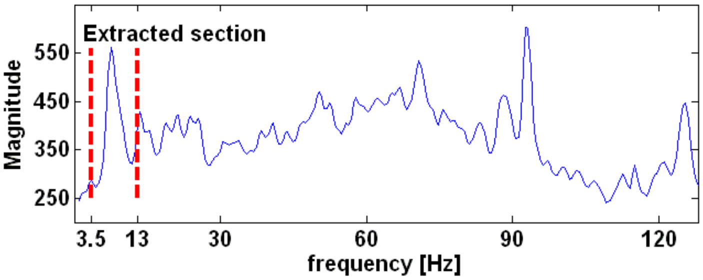

Figure 12. Extracted candidate spectrum of unchanged scenario.

The plots in Figure 13 show the correlation coefficients of two candidate spectrums compared against the unchanged reference spectrum. The correlation for the unchanged candidate has a strong peak at the zero shift location, indicating that it matches the reference spectrum. The peak in the correlation for the changed candidate spectrum is at a shifted location.

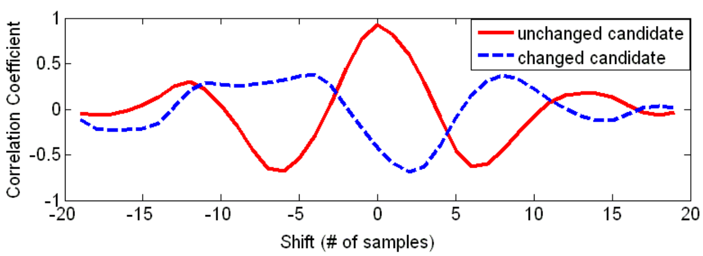

Figure 13. Cross correlation between candidates for the unchanged and changed scenario (SC3) with respect to the unchanged reference spectrum.

5 RESULTS AND DISCUSSION

The proposed detection approach was tested using a data set generated with the experimental setup previously described. We now show some of the preliminary findings of this approach and the corresponding results.

5.1 *Dataset.*

Our dataset consists of 60 acceleration signals from each of the five sensors (front suspension, back suspension, left wheel, right wheel, and bridge) collected under four different change scenarios (unchanged, +6 kg, +10 kg, +14 kg) and vehicle speeds (1 m/s, 1.5 m/s, 2 m/s 2.5 m/s 3 m/s). The signals were sampled at 256 Hz and vary in length from 1 to 3 seconds. The variation in signal length occurs because of the time it takes the vehicle to travel over the bridge at different speeds.

5.2 *Experimental Setup.*

To evaluate our classification system, we performed a series of cross-validation experiments. We first fixed a group size, N = 3, 4, …, 35. For each speed and each sensor, we randomly selected 20 signals from the undamaged bridge and used them as our training set. We then randomly selected N signals from each of the changed scenarios and used them to form test sets. Additionally, we selected N of the remaining 40 signals from the unchanged scenario and formed a test set with them. This random selection was repeated in a 1,000-fold validation.

For each scenario, we report the detection rate as the percentage of folds in which the test set was labeled as changed. For the three changed scenarios, the detection rate represents the true positive rate (TPR), while for the unchanged bridge, it represents the false positive rate (FPR). A perfect system would have a TPR of 1 for each damage condition and a FPR of 0.

5.3 *Results and Discussion.*

Figure 14 shows the damage detection rate for each scenario and sensor location plotted across speed, with N=35. The four lines represent the detection rate for the undamaged bridge and for each of the three damage scenarios. Ideally, we would see the FPR of 0 for the undamaged bridge, and the TPR of 1 for each of the damage scenario.

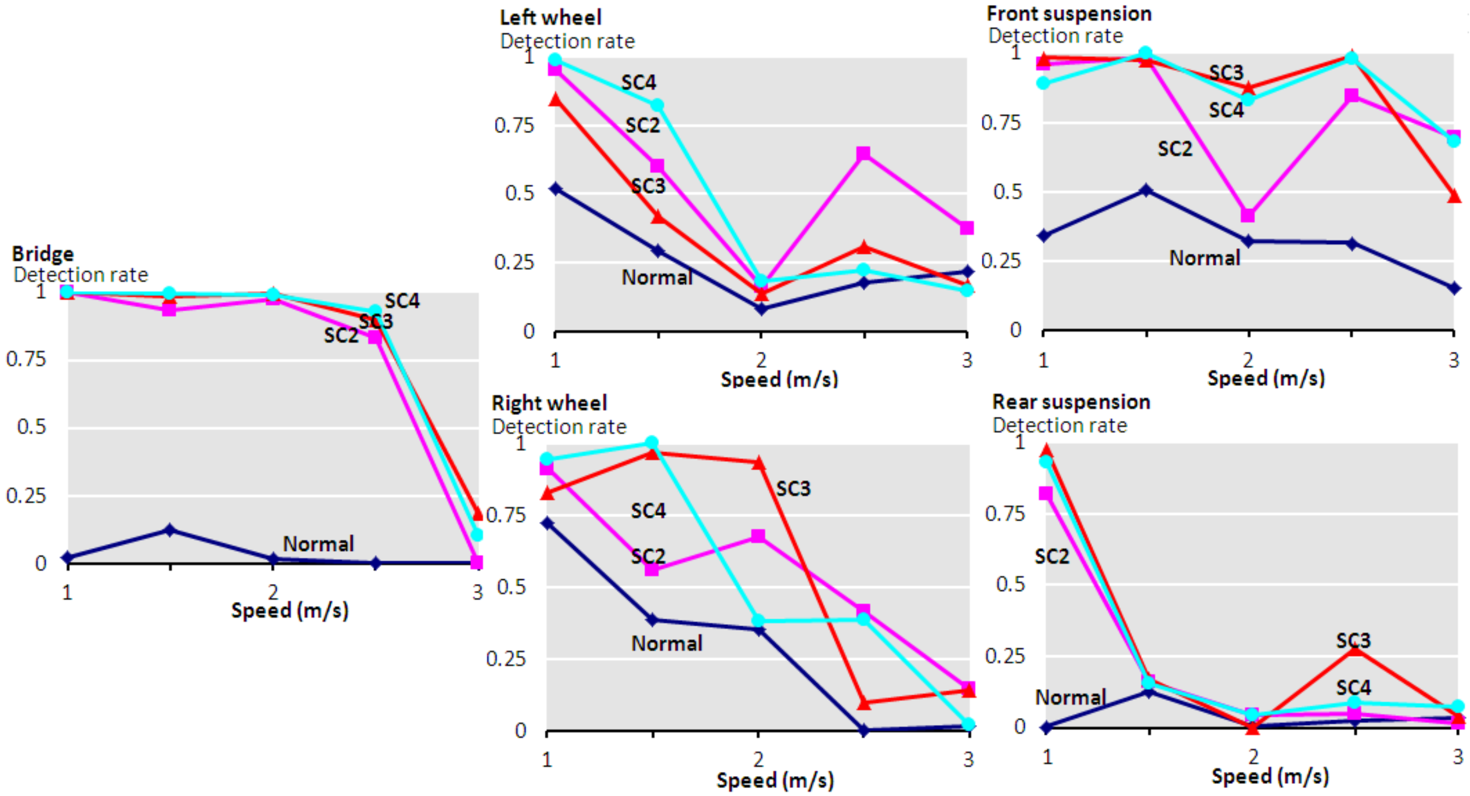

Figure 14. Detection rate for each scenario and sensor location plotted across speed, averaging 35 runs. For each damage scenario, the curve represents the true positive rate (TPR), while for the normal (undamaged) case, the curve represents the false positive rate (FPR). Accuracy is consistently good at the lowest speed, with the sensors on the suspension providing the best accuracy of the indirect sensors.

The lowest speed consistently produces the best detection for all sensors, while the accuracy for other speeds is inconsistent across sensors. This may be due to increased noise or shorter signal duration (which reduce the effectiveness of our spectrum averaging technique) for higher speeds. The sensor on the bridge detects damage nearly perfectly, validating our classification technique for the easier, direct-monitoring case. Of the indirect sensors, those on the suspension were better than those on the wheel. This is likely because the suspension acts as a low-pass filter, reducing the noise while preserving the low fundamental frequency of the bridge.

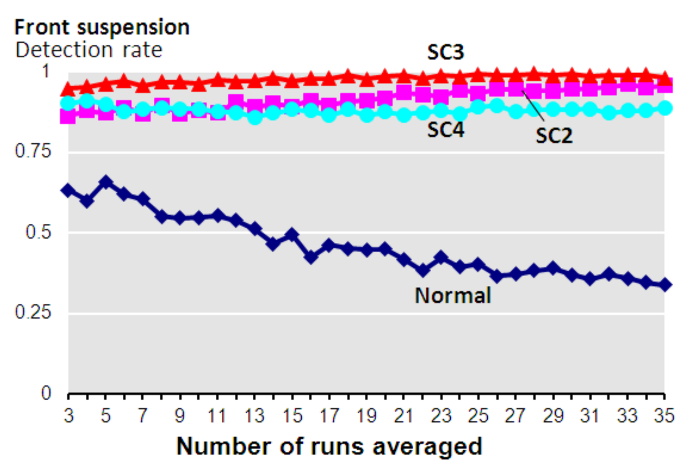

Figure 15.The effect of the number of averaged runs on the detection rate for the front suspension sensor at a speed of 1 m/s. Averaging a larger number of runs increases the TPR, while lowering the FPR.

Figure 15 shows the effect of N on the classification accuracy for the front suspension sensor at 1 m/s. In general, accuracy increases as N increases. For some sensors and speeds, there was a clear diminishing-returns effect, while for others there was not. Contrary to what we would expect, scenario 4 is not consistently the easiest to detect. Inspection of the spectra reveal that the peak for the fundamental frequency appears wider and shorter as more mass is added to the bridge, decreasing the accuracy of the correlation matching method.

6 CONCLUSIONS AND FUTURE WORK

This paper presents initial work for detecting changes in bridge structures based on acceleration data from passing vehicles. We refer to this approach as *indirect*. We compare the results of the *indirect* with the traditional *direct* approach in which sensors are located on the bridge structure.

An experimental setup that resembles a moving vehicle passing over a simply supported bridge was used to generate dynamic interaction data from several physical scenarios. The scenarios consisted of changes in the mass of the bridge structure generated by adding a localized mass at midspan.

A detection procedure was developed to capture the shifts in the fundamental frequency of the bridge.

The detection capability of the proposed signal processing approach is more stable across different speeds for acceleration data gathered in a *direct* fashion rather than in the *indirect one.*

For the particular experimental setup used in this work and the different scenarios simulated, the sensor location on the vehicle has a strong influence in terms of the detection capability of the different scenarios. The sensor located at the front of the vehicle over the suspension system outperformed those of all other sensor locations.

Lower travelling speeds of the vehicle seem to be better for identifying changes in the natural frequency of the bridge than higher traveling speeds.

Regarding the number of runs averaged to calculate the true positive detection rate (TPR), there is a mild linear increasing trend over the quality of the detection. More significant is the reduction of false positive rate when increasing the number of runs.

Future work will include an exploration of the sensitivity of the approach to smaller changes in the bridge structural system.

We are also interested in examining the consistency of the TPR trends across different speeds. We will study this by populating our experimental data with smaller speed intervals.

We will also explore other types of changes that resemble damage scenarios in a real bridge structure. Such scenarios will consider frozen bearings and cracks. The first will be modeled by increasing the rotational restraint at the supports of the simply supported bridge. The latter will be simulated by a section reduction of the supporting beam elements of the bridge.

7 ACKNOWLEDGMENTS

This research was supported by a grant of the National Science Foundation (Award No. CMMI1130616) and by the Traffic 21 initiative at Carnegie Mellon University. We are grateful for this support. We also thank Ranny Zhao and Colin Rutenbar, who participated in the construction of the experimental setup.

8 REFERENCES

Cerda F., Garrett J., Bielak J., Bhagavatula R. & Kovačević J. 2010. Exploring Indirect Vehicle-Bridge interaction for SHM. *Proceedings of the Fifth International Conference on Bridge Maintenance, Safety and Management,* IABMAS2010, Philadelphia, USA, 696-702.

Kim, C.W. Kawatani, M. & Fujimoto T, (2010), Identifying bending stiffness change of a beam under a moving vehicle, *Proceedings of the Fifth International Conference on Bridge Maintenance, Safety and Management,* IABMAS2010, Philadelphia, USA, 761-767.

Lin, C.W., & Yang Y.B. 2005. Use of a passing vehicle to scan the fundamental bridge frequencies: An experimental verification. *Engineering Structures* 27, no. 13 (November): 1865-1878.

Yang, Y. B., Lin C. W., & Yau J. D. 2004. Extracting bridge frequencies from the dynamic response of a passing vehicle. *Journal of Sound and Vibration* 272, no.3-5(May 6):471-493.